DR XINGGUO YE (Orcid ID : 0000-0002-6616-2753)

DR SHUANGHE CAO (Orcid ID : 0000-0002-2905-0728)

Article type : Regular Manuscript

TaVrt2, an SVP-like gene, cooperates with *TaVrn1* to regulate vernalization-induced flowering in wheat

Li Xie[1], Yong Zhang[1], Ke Wang[1], Xumei Luo[1], Dengan Xu[1], Xiuling Tian[1], Lingli Li[1], Xingguo Ye[1], Xianchun Xia[1], Wenxue Li[1], Liuling Yan[2] and Shuanghe Cao[1]*

[1]Institute of Crop Sciences, Chinese Academy of Agricultural Sciences, Beijing 100081, China

[2]Department of Plant and Soil Sciences, Oklahoma State University, Stillwater, OK 74078, USA

Corresponding author e-mail: caoshuanghe@caas.cn; Tel: +86-10-82108610; ORCID: 0000-0002-2905-0728;

Received: 22 October 2019

Accepted: 19 November 2019

Summary

- *TaVrn1*, encoding a MADS-box transcription factor (TF), is the central regulator of wheat vernalization-induced flowering. Considering that the MADS-box TF usually works by forming hetero or homo dimers, we conducted yeast two hybrid screening and identified an SVP-like MADS-box protein TaVrt2 interacting with TaVrn1. However, the specific function of TaVrt2 and the biological implication of its interaction with TaVrn1 remained unknown.
- We validated the function of TaVrt2 and TaVrn1 by wheat transgenic experiments and their interaction through multiple protein-binding assays. Population genetic analysis was also used to display their interplay. Transcriptomic sequencing and chromatin immunoprecipitation assays were performed to identify their common targets.
- TaVrt2 and TaVrn1 are flowering promoters in the vernalization pathway and interact physically *in vitro*, *in planta* and in wheat cells. Additionally, *TaVrt2* and *TaVrn1* were significantly induced in leaves by vernalization, suggesting their spatio-temporal interaction during vernalization. Genetic analysis indicated that *TaVrt2* and *TaVrn1* had significant epistatic effects on flowering time. Furthermore, native *TaVrn1* was up-regulated significantly in *TaVrn1*-OE (overexpression) and *TaVrt2*-OE lines. Moreover, TaVrt2 could bind with *TaVrn1* promoter directly.
- A *TaVrt2*-mediated positive feedback loop of *TaVrn1* during vernalization was proposed, providing additional understanding on the regulatory mechanism underlying vernalization-reduced flowering.

Key words: feedback loop; flowering time; SVP; TaVrn1; TaVrt2; vernalization; wheat

Introduction

Wheat (*Triticum aestivum*) is the most widely grown staple crop due to its wide adaptation (FAO, https://www.idrc.ca/en/article/facts-Fig.s-food-and-biodiversity). Based on the requirement or not for cold temperature to promote flowering, wheat cultivars are classified into winter and spring types. This requirement for cold known as vernalization, prevents temperate plants from flowering under freezing winter conditions (Kim et al., 2009). Wheat cultivars grown in different environments need diverse vernalization characteristics to ensure flowering and reproductive development at an optimum time, which is critical for high yield and crop rotation (Milec et al., 2009).

Vernalization-controlled flowering in wheat is mainly determined by four loci, *TaVrn1*, *TaVrn2*, *TaVrn3*, and *TaVrn4* that have been positionally cloned; *TaVrn4* was identified as a duplication of *TaVrn1* (Yan et al., 2003; Yan et al., 2004a; Yan et al., 2006; Kippes et al., 2015). *TaVrn1* acts as a flowering promoter. In winter wheat, *TaVrn1* is barely expressed before vernalization, but is strongly induced by vernalization and maintains high expression levels under warm temperatures after vernalization (Trevaskis et al., 2003; Yan et al., 2003). Subsequent studies showed that vernalization decreased the epigenetic repression mark H3K27me3 and increased epigenetic activation mark H3K4me3 at the *TaVrn1* locus (Oliver et al., 2009; Diallo et al., 2012). The altered chromatin status of *TaVrn1* is maintained after vernalization, likely conferred as an epigenetic memory of vernalization (Oliver et al., 2009; Diallo et al., 2012). Vernalization induces TaGRP O-GlcNAcylation, release *TaVrn1* pre-mRNA from the binding of TaGRP and consequently promotes the maturity and processing of the pre-mRNA (Xiao et al., 2014; Xu et al., 2018). *TaVrn2* encodes two redundant ZCCT proteins (ZCCT1 and ZCCT2), which repress flowering (Yan et al., 2004a), whereas *TaVrn3* is a *FLOWERING LOCUS T*-like gene and promotes flowering (Yan et al., 2006). *TaVrn1* is a direct target of vernalization and acts as the upstream regulator of *TaVrn2* and *TaVrn3*. TaVrn1 directly binds to the *TaVrn2* promoter to repress its expression (Yan et al., 2004b; Chen and Dubcovsky, 2012; Deng et al., 2015). *TaVrn1* also eliminates the repression of *TaVrn2* on *TaVrn3* allowing *TaVrn3* to promote flowering (Li et al., 2011). Moreover, a study in barley (*Hordeum vulgare*) suggested that HvVrn1 directly binds to the *HvVrn3* promoter and activates its expression (Deng et al., 2015). Hence, *TaVrn1* is the central regulator in the vernalization flowering pathway.

TaVrn1 encodes a MADS-box protein highly homologous to *AP1*, a floral meristem identity gene

in *Arabidopsis* (Mandel et al., 1992; Danyluk et al., 2003; Trevaskis et al., 2003; Yan et al., 2003). MADS-box proteins usually work by forming hetero or homo dimers (de Folter et al., 2005; Kaufmann et al., 2005). Hence, it is helpful to dissect the function of TaVrn1 in the interaction with MADS-box proteins. We previously performed a yeast two hybrid screening and identified a Short Vegetative Phase (SVP)-like MADS-box transcription factor (TF) TaVrt2 as a partner of TaVrn1 (Cao and Yan, 2013). SVP inhibits flowering by interacting with another MADS-box protein, FLC, in *Arabidopsis* (Hartmann et al., 2000; Li et al., 2008). In wheat, *TaVrt2* was also initially regarded as a flowering repressor and its transcription was repressed by vernalization (Kane et al., 2005; Kane et al., 2007). Binding of TaVrt2 directly to the CArG box in the *TaVrn1* promoter is considered to be essential for the repression of *TaVrn1* before vernalization (Kane et al., 2007). However, a series of subsequent studies showed that *TaVrt2* and *HvVrt2* (the orthologue in barley) was induced by vernalization (Trevaskis et al., 2007; Dubcovsky et al., 2008; Winfield et al., 2009; Li et al., 2017), which was contrary to previous research. Thus, it is necessary to uncover the specific function of TaVrt2 and the biological implication of its interaction with TaVrn1 in the vernalization-regulated flowering pathway.

In the present study, we verified *TaVrt2* as a flowering promoter in the vernalization regulatory pathway through transgenic experiments. Physical interaction between TaVrt2 and TaVrn1 was confirmed using multiple protein-binding assays. Genetic interplay between *TaVrt2* and *TaVrn1* was also detected in a segregating population derived from a cross between their overexpression lines. Transcriptomic analyses and ChIP-qPCR assays revealed that the TaVrt2/TaVrn1 protein complex bound to the promoter of *TaVrn1* to promote its expression. Finally, a model that *TaVrt2* and *TaVrn1* orchestrated flowering in the vernalization pathway was proposed.

Materials and Methods

Plant materials and growth conditions

Three elite Chinese winter wheat cultivars Kenong199 (KN199), Jimai22 and Zhongmai175 were used to investigate the transcriptional patterns of *TaVrt2* and *TaVrn1*. KN199 and Jimai22 are semi-winter or weak winter-habit wheat cultivars, grown in the Yellow-Huai River Valley Winter Wheat Zone (Northern latitude: 36~39^{o}), the largest wheat growing region, whereas Zhongmai 175 is a strong winter-habit wheat released in the Northern China Winter Wheat Zone (Northern latitude: 39~41^{o}). KN199, which needs approximately 30 d of cold exposure to fully satisfy its vernalization requirement, was used as the recipient of wheat transgenic experiments. An F_2

population for study of genetic interaction between *TaVrn1* and *TaVrt2* were produced from a cross of over-expression lines *TaVrt2*-L25 and *TaVrn1*-L13. The plants with different genotypes in the F_2 population were identified and included NC (transgenic null), H-*TaVrt2* (*TaVrn1*-OE), H-*TaVrn1* (*TaVrt2*-OE), and H-*TaVrn1*+*TaVrt2* (double OE) lines. The spring wheat cultivar Ningchun4 was used to compare with *TaVrn1*-OE lines for the *TaVrn1* expression level.

Wheat materials were grown in a growth chamber set at 15-18°C (normal growing temperature), and a photoperiod of 16 hours (h) light / 8 h darkness. For vernalization, three-week old seedlings were moved to a cold room at 2-4°C. *N. benthamiana* used in luciferase complementation imaging (LCI) assays was planted in a growth chamber at 20-23°C with the same photoperiod as above.

Genetic transformation and flowering time measurement

The *TaVrt2-7DS* (GenBank accession number: AAY43789) and *TaVrn1-5AL* (GenBank accession number: JQ915056) were isolated from a strong winter-habit wheat line 2174, and their encoding proteins were proved to interact with each other in yeast (Cao and Yan, 2013). Their full-length coding sequences (CDS) with or without stop codons was cloned into the entry vector pDONR207 and then recombined into the destination construct (pUbiGW) according to the handbook of Gateway cloning (Invitogen). A pUbiGW expression vector with the *YFP* gene and *HA* tag, a ZmUbi promoter-driven overexpression vector compatible with the Gateway cloning system was produced and constructs were transformed into *Agrobacterium tumefaciens* strain EHA105 (Biomed) by the freeze-thawing method according to the product manual (Biomed). Wheat transformation was performed by infecting immature embryos of KN199 with EHA105 carrying the destination constructs (Ishida et al., 2015).

More than 10 plants were measured for each line and flowering time for each plant was recorded when the primary spike was fully emerged from flag leaf sheath.

Pulldown

The above *TaVrt2-7DS* and *TaVrn1-5AL* CDS were inserted into pGEX-4t-1 (GE) and pMAL-5cx (NEB) vector, respectively, and transformed into *E. coli* BL21(DE3) (TRANSGENE). The resulting proteins were expressed and extracted according to the procedures in the instruction manual (NEB; GE). Mixtures of 10 mg of TaVrt2-GST and 10 mg TaVrn1-MBP proteins in 1 ml lysis buffer (150 mM KCl, 20 mM HEPES, 5 mM $MgCl_2$, 10% glycerol, 1 mM DTT, 1 mM PMSF, 0.5 mM EDTA) were incubated at 4°C for 2 h. Sixty µl of amylase resin (NEB) was added

into the above mixtures and shaken at 4°C for 1 h. The resin was washed 5 times using lysis buffer and then eluted using 80 μl elution buffer (lysis buffer containing 10 mM maltose). The isolated proteins were separated in 12% SDS-PAGE gels and detected by coomassie brilliant blue staining and Western blotting with anti-GST antibody (Abmart, 1:5000 dilution).

Luciferase complementation imaging (LCI)

The LCI assay was performed as described previously (Sun et al., 2013). The above *TaVrt2-7DS* and *TaVrn1-5AL* CDS were cloned into pCAMBIA1300cLUC and pCAMBIA1300nLUC vectors, respectively. *N. benthamiana* leaves were infiltrated by *Agrobacterium tumefaciens* strain GV3101 (Biomed) carrying the target construct. LUC activities in leaves were measured 50 h after infiltration. Fluorescence was monitored and imaged using LB985 NightSHADE (Berthhold Technologies) shortly after 100 μl of luciferase assay substrate (Promega) were sprayed on to the infiltrated leaves.

Bimolecular fluorescence complementation (BiFC)

For BiFC assays, full-length CDS of *TaVrt2-7DS* and *TaVrn1-5AL* were cloned into pUC-SPYNE(R)173 and pUC-SPYCE(M), respectively (Waadt et al., 2008). The constructs were transformed into wheat protoplasts following Shan et al. (2014). Fluorescence signals of yellow fluorescent protein (YFP) was observed and imaged using a laser confocal microscope (Zeiss LSM700) 15 h after transformation.

RNA extraction and reverse transcription quantitative PCR (qPCR)

Fresh samples were harvested and quickly frozen by liquid nitrogen. Total RNA was extracted using an EasyPure Plant RNA Kit (TRANSGENE) according to the manufacturer's instructions and used to generate cDNA with a PrimeScript RT Reagent Kit plus gDNA Eraser (Takara). qPCR was performed on cDNA samples produced from three biological replicates in a BioRad CFX system using iTaq Universal SYBR Green Supermix (BioRad) following the manufacturer's protocol. For relative quantification, gene expression was calculated by the $2^{-\Delta\Delta Ct}$ method (Schmittgen and Livak, 2008). The wheat *actin* gene (accession: *AB181991*) was used as the internal control to calibrate the expression levels of genes of interest. For absolute quantification, standard curves for each primer pair were constructed using a gradient dilution series of genomic DNA (gDNA) (9 ng/μl, 3 ng/μl, 1 ng/μl, 0.33 ng/μl, 0.11 ng/μl, 0.033 ng/μl) from KN199 (Cao et al., 2011). The absolute amounts of target genes were calculated by the standard curves and further

normalized by the *actin* gene.

RNA-seq

Two lines of each of *TaVrt2*-OE (*TaVrt2*-L1, *TaVrt2*-L35), *TaVrn1*-OE (*TaVrn1*-L5, *TaVrn1*-L8) and TNL [*TaVrt2*-L35(-), *TaVrn1*-L5(-)] were used for RNA-seq. Samples with three biological replications were collected from both the transgenic lines of the gene of interest and their transgenic negative lines (TNL). Fresh leaves from five individuals in each line were collected on the 15th day after the 10-day vernalization period for RNA extraction. RNA isolation and sequencing were performed by Novogene, Beijing. Ten Gb of transcriptomic data for each sample was obtained from the Illumina HiSeq 4000 platform. Deseq (DESeq R package 1.18.0) was used to analyze differential expression. Genes with an adjusted *P*-value <0.05 and fold change (FC) value ≥2 (|Log2 FC| ≥1) between contrasting groups were considered to be differentially expressed.

ChIP-qPCR

ChIP was performed following Luo and Lam (2014). In brief, 1 g of leaf tissue was ground in liquid nitrogen and resuspended by 30 ml nuclear isolation buffer (10 mM HEPES pH 7.6, 400 mM sucrose, 5 mM KCl, 5 mM $MgCl_2$, 5 mM EDTA, 1% formaldehyde, 14 mM 2-mercaptoethanol, 0.6% Triton X-100, and 0.4 mM PMSF). The lysate was crosslinked at room temperature for 10 min and was stopped by adding 2 ml 2 M glycine. The lysate was filtered into a new tube. Nuclei were pelleted by centrifuging at 2,800 *g* for 10 min and dissolved in 200 µl nuclear lysis buffer (50 mM Tris–HCl pH 7.5, 1 % SDS, 10 mM EDTA pH 8.0). The nuclei extract was loaded into sonicator (Bioruptor UCD200) and sonicated at 30 s on/60 s off for 5 times. The sheared chromatin was centrifuged at 16,000 *g* for 5 min and the supernatant was transferred to a new tube. Thirty µl protein A+G magnetic beads (Merck) together with 2 µg target antibody (anti-GFP, Abcam; anti-H3K4me3, Merck; anti-H3K27me3, Merck) or 2 µg IgG antibody as the negative control was added to the tube, and the mixture was shaken overnight at 4°C. After incubation, the beads were successively washed by: 1 ml low salt immune complex wash buffer (0.1% SDS, 1.0% TritonX-100, 2 mM EDTA, 20 mM Tris-HCl pH 8.0, 150 mM NaCl), 1 ml high salt immune complex buffer (0.1% SDS, 1.0% TritonX-100, 2 mM EDTA, 20 mM Tris-HCl pH 8.0, 500 mM NaCl), 1 ml LiCl immune complex wash buffer (0.25 M LiCl, 1.0% NP-40, 1% sodium dexycholate, 1 mM EDTA, 10 mM Tris-HCl pH 8.0), and 1 ml TE then eluted by 200 µl elution buffer (1% SDS, 100 mM $NaHCO_3$). The eluted immune complex was

incubated at 65°C overnight together with 8 µl 5 M NaCl followed by 1 µl proteinase (Fermentas) for 2 h at 50°C. The immunoprecipitated DNA was purified and then quantified by qPCR, which was performed on ChIP samples collected from three biological replicates in a BioRad CFX system using iTaq Universal SYBR Green Supermix (BioRad) following the manufacturer's user manual. The enrichment of co-immunoprecipitated DNA was calculated by the $2^{-\Delta\Delta Ct}$ method (Schmittgen and Livak, 2008). The relative enrichment folds of co-immunoprecipitated DNA was calculated by normalization with the IgG control, and then calibrated with TNL or non-vernalized lines. All primers used in the study are listed in **Table S1**.

Statistical analysis

The effect of epistatic interaction of *TaVrt2* and *TaVrn1* on flowering time in KN199 was analyzed by two-way ANOVA (Mo et al., 2018). The Proc General Linear model (GLM) was used to estimate significance of effects (P<0.05). Differences in *TaVrn1* expression among KN199, Ningchun4 and transgenic lines were assessed by Duncan's multiple range tests. Differences in flowering time, gene expression and chromatin enrichment between transgenic (*TaVrt2*-OE or *TaVrn1*-OE lines) and NC (including TNL and KN199) were compared by the Student's *t* tests. The average and SD (standard deviation) of all data were calculated in Excel 2013 (www.microsoft.com). All statistical analyses were conducted using SAS 9.4 (www.sas.com) or Excel 2013.

Results

***TaVrt2* is a flowering promoter in the vernalization regulatory pathway**

To determine the function of *TaVrt2* (GenBank accession number: AAY43789) in vernalization-induced flowering, we overexpressed *TaVrt2* in the winter wheat cultivar Kenong199 (KN199) by *Agrobacterium*-mediated transformation. Thirty-five positive transgenic lines were identified by PCR; six lines with relatively high expression levels of transformed *TaVrt2*, were chosen as the representatives of *TaVrt2* overexpression lines for further analyses **(Fig. S1)**. We investigated and compared the flowering times of these positive transgenic lines with negative controls (NC) including KN199 and transgenic null lines (TNL). The positive transgenic lines had similar flowering times to NC when vernalized for 30 days (d) **(Fig. 1)**, whereas they flowered significantly earlier than NC under non- and incomplete (10 days) vernalization conditions **(Fig. 1)**. On average, the positive lines flowered 6.2 d and 5.4 d earlier than NC when vernalized for 0 d

or 10 d, respectively **(Fig. 1)**, indicating that *TaVrt2* is a flowering promoter in the vernalization pathway.

TaVrt2 physically binds to TaVrn1

Previous yeast two hybrid (Y2H) results showed that TaVrt2 could interact with TaVrn1, the core regulator in the vernalization flowering pathway (Kane et al., 2005; Cao and Yan, 2013). Considering the high false positive rate of Y2H, we conducted multiple assays to further verify interaction between TaVrt2 and TaVrn1. We firstly performed a pulldown experiment *in vitro* using MBP-tagged TaVrn1 and GST-tagged TaVrt2. Western blotting showed that TaVrn1 could bind with TaVrt2 **(Fig. 2A)**. To assess whether TaVrt2 and TaVrn1 can interact *in planta*, we employed a luciferase (LUC) complementation imaging (LCI) assay in *Nicotiana benthamiana* leaves. Significant LUC signals were detected in the area where TaVrt2-cLUC and TaVrn1-nLUC were co-infiltrated, whereas no LUC signals were observed in the negative control **(Fig. 2B)**. This interaction was also validated by a bimolecular fluorescence complementation (BiFC) assay in wheat protoplasts. The fluorescence signal was detected in cell nuclei of protoplasts carrying TaVrt2-cYFP and TaVrn1-nYFP, whereas no signal was observed in those carrying control constructs, TaVrt2-cYFP+nYFP or cYFP + TaVrn1-nYFP **(Fig. 2C)**. Collectively, TaVrt2 and TaVrn1 interact with each other *in vitro*, *in planta* and in wheat cells.

***TaVrt2* and *TaVrn1* overlap in spatio-temporal expression pattern during vernalization**

To determine whether *TaVrt2* and *TaVrn1* overlap spatially in wheat, we investigated their expression patterns in different tissues, including leaves, roots, stems, florets, young spikes and immature grains. Transcriptional analyses showed that *TaVrn1* was highly expressed in all tissues except in roots, whereas *TaVrt2* was mainly expressed in the leaves and stems (**Fig. 3A**). Importantly, both *TaVrt2* and *TaVrn1* were highly expressed in leaves and stems, the major tissues responsible for vernalization perception, indicating that their expression overlapped spatially.

TaVrn1 was reported as the central component in the vernalization-regulated flowering pathway and is strongly induced by vernalization (Trevaskis et al., 2003, Yan et al., 2003). To further identify whether *TaVrt2* and *TaVrn1* interplay in the vernalization process, we investigated dynamic changes in responses of *TaVrt2* and *TaVrn1* to vernalization in three winter wheat cultivars (KN199, Jimai22 and Zhongmai175). Schematics of treatments and sampling time-points of the experimental materials are shown in **Fig. 3B**. Transcriptional pattern assays showed that

TaVrt2 and *TaVrn1* had differential expression responses to vernalization **(Fig. 3C)**. In all three cultivars, *TaVrt2* expression level increased rapidly during vernalization and sharply declined after vernalization, whereas the expression level of *TaVrn1* increased moderately at the beginning of vernalization and then greatly increased after 3 weeks of vernalization. Unexpectedly, *TaVrn1* expression decreased in Zhongmai175 and Jimai22 and only slightly increased in KN199 immediately after vernalization. We also investigated the transcriptional patterns of *TaVrn1* and *TaVrt2* in samples from non-vernalized plants; their expression slowly increased with plant development. Notably, both *TaVrt2* and *TaVrn1* were obviously induced during vernalization, supplying a time course for their interaction.

In addition to *TaVrt2*, *WM22* and *WM28* were other two *SVP*-like genes in wheat (**Fig. S2A**). To investigate whether the two paralogous genes are also involved in vernalization regulation, we investigated their expression during vernalization. qPCR results showed that both *WM22* and *WM28* had a similar expression pattern with *TaVrt2*, viz. induced during vernalization, and declined significantly after vernalization **(Fig. S2B)**. However, the expression levels of *WM22* and *WM28* were only slightly increased in vernalization conditions. Among them, the expression level of *TaVrt2* was lowest among the three genes before vernalization, but sharply increased to be highest during vernalization (**Fig. S2B**).

TaVrt2 and *TaVrn1* interact genetically

We overexpressed *TaVrn1* in KN199 to further investigate the relationship between *TaVrt2* and *TaVrn1*. Fifteen independent *TaVrn1*-OE lines were generated; four lines with higher *TaVrn1* expression activity flowered 4-7 d earlier than NC after a 10-day vernalization period, confirming that *TaVrn1* is a flowering promoter in the vernalization-regulated pathway **(Fig. S3B and S3C)**. However, *TaVrn1* overexpression did not greatly accelerated flowering. qPCR assays showed that *TaVrn1* expression levels in the transgenic lines were 40-120 fold higher than NC (including KN199 and TNL), but still much lower than the spring wheat cultivar Ningchun4, which was 400-fold higher than NC **(Fig. S3A)**. Additionally, the allele of *TaVrn1* for transgenic assays, which was used as "prey" to perform Y2H screening in Cao and Yan (2013), was isolated from a strong winter-habit cultivar 2174 and might not be a high-activity one to promote flowering. Furthermore, KN199, is a weak or semi-winter wheat and has comparatively high expression levels of native *TaVrn1* (**Fig. 3C**), which could overshadow the effect of the transgenic *TaVrn1* on flowering time. In all, the above speculations may account for the moderate promotion effect on

flowering in the *TaVrn1*-OE lines.

We created an F_2 population from a cross between a *TaVrt2*-OE line and a *TaVrn1*-OE line, and identified *TaVrt2*-OE, *TaVrn1*-OE, their double OE lines and TNL, designated as H-*TaVrt2*, H-*TaVrn1*, H-*TaVrt2*+*TaVrn1* and NC, respectively. qPCR assays showed that overexpressed *TaVrt2* and *TaVrn1* in H-*TaVrt2*+*TaVrn1* lines had similar expression levels to the counterparts in H-*TaVrt2* and H-*TaVrn1* lines, respectively **(Fig. 4A)**. The phenotypic differences between the transgenic lines and their TNL are consistent regardless of under 10-d vernalization or NV conditions. Compared to NV, 10-day vernalization can promote flowering of NC, TaVrn1-OE, TaVrt2-OE and their double OE lines, facilitating to get phenotypic data earlier. Additionally, individual plants in each line have more consistent flowering time under 10-d vernalization conditions than under NV conditions, facilitating to investigate the phenotypic data. Thus, we selected the 10-day vernalization condition to conduct expression analyses for further analysis of *TaVrt2*-OE, *TaVrn1*-OE, their double OE lines and TNL. Phenotypic investigation displayed that the H-*TaVrt2*, H-*TaVrn1* and H-*TaVrt2*+*TaVrn1* lines flowered 2.4, 4.2 and 9.7 d earlier, respectively, than the NC under incomplete (10-day) vernalization conditions **(Fig. 4B and 4C)**. Two-way analysis of variance (ANOVA) showed a significant epistatic effect ($P < 0.05$) on flowering time between *TaVrt2* and *TaVrn1* **(Fig. 4B)**.

***TaVrn1* is a common target of TaVrt2 and TaVrn1**

To further dissect the regulatory mechanism of *TaVrt2* and *TaVrn1* in vernalization-induced flowering, we performed RNA-seq using the leaves of *TaVrt2*-OE, *TaVrn1*-OE and TNL on the 15th day after the 10-day vernalization treatment (V10N15), the key time point in transition from the vegetative to reproductive phases. In total, 1,107 and 1,965 differentially expressed genes (DEGs) were identified in the *TaVrt2*-OE and *TaVrn1*-OE lines, respectively, compared with TNL **(Fig. 5A; Dataset S1)**; 519 genes were common, indicating that *TaVrt2* and *TaVrn1* had a large proportion of overlapping downstream targets at the initial stage of flowering.

Notably, *TaVrn1-5DL* (the chromosome 5DL member of *TaVrn1*) expression was significantly up-regulated in both *TaVrt2*-OE lines [Fold change (FC) = 5.28; $P = 0.0059$] and *TaVrn1*-OE lines (FC = 4.14, $P = 0.0053$) compared to TNL **(Dataset S1)**. qPCR confirmed that the *TaVrt2*-OE and *TaVrn1*-OE lines had significantly higher expression levels of *TaVrn1-5DL* than TNL **(Fig. 5B)**. *TaVrn1-5DL* is induced by vernalization **(Fig. 5B; Dataset S1)** and the TaVrt2/TaVrn1 complex mainly functions during vernalization **(Fig. 3C)**. Thus *TaVrn1-5DL* is very likely a regulatory

target of the TaVrt2/TaVrn1 complex in the vernalization-mediated flowering pathway. We also investigated the expression of native *TaVrn1-5AL* and *TaVrn1-5BL* genes in the transgenic lines and TNL, and found that native *TaVrn1-5AL* was up-regulated in both *TaVrt2*-OE and *TaVrn1*-OE lines (**Fig. 5B and 5C**). However, *TaVrn1-5AL* had less increase than *TaVrn1-5DL* **(Fig. 5C)**. In contrast, *TaVrn1-5BL* was hardly detected in both transgenic lines and TNL. Genotyping of the *TaVrn1* alleles in KN199 showed that KN199 had recessive alleles at both the *TaVrn1-5AL* and *TaVrn1-5BL* loci, and a dominant allele at *TaVrn1-5DL* based on the gene-specific markers **(Fig. S4; Table S2)** (Zhang et al., 2008). The recessive *TaVrn1* alleles had complete VRN boxes and first intron, considered to be essential for the repression of *TaVrn1* expression, hence their expression should be inhibited under incomplete vernalization conditions (Yan et al., 2004a; Fu et al., 2005; Distelfeld et al., 2009), probably accounting for different responses of the *TaVrn1* alleles to *TaVrt2* and *TaVrn1* overexpression. As such, each of *TaVrn1* and *TaVrt2* can promote expression of all *TaVrn1* orthologues, *TaVrn1-5AL* and *TaVrn1-5BL* and *TaVrn-5DL,* if excluding their genotypic variations.

TaVrt2 and _TaVrn1_ have epistatic effects on _TaVrn1_ expression

To further assess whether and how interaction between TaVrt2 and TaVrn1 regulates *TaVrn1* expression, we compared the expression of *TaVrn1-5DL*, as a representative of *TaVrn1*, in NC, H-*TaVrt2*, H-*TaVrn1* and H-*TaVrt2*+*TaVrn1* lines from the above genetic population. Leaf samples were collected at three developmental stages: before vernalization (V0), 10th day of vernalization (V10) and 5 days after the 10-d vernalization period (V10N5). Expression of *TaVrn1-5DL* in H-*TaVrt2*, and H-*TaVrn1*, were significantly higher than NC at V10N5, consistent with the above RNA-seq and qPCR results, but not significantly different from that of NC at V0 or V10, probably due to insufficient TaVrn1 and TaVrt2 proteins to form a TaVrt2/TaVrn1 complex in the H-*TaVrt2* and H-*TaVrn1* lines **(Fig. 5B and 5D; Dataset S1)**. In contrast, the expression level of *TaVrn1-5DL* in H-*TaVrt2*+*TaVrn1* was significantly higher than the NC, H-*TaVrt2* and H-*TaVrn1* lines at all three stages, indicating that TaVrt2 and TaVrn1 can promote *TaVrn1-5DL* expression when combined.

TaVrt2 directly binds to the promoter of _TaVrn1_

Previous studies showed that TaVrt2 physically binds to the CArG-box in the promoter of *TaVrn1* (Kane et al., 2007; Dubcovsky et al, 2008). To further test this *in vivo*, we performed ChIP-qPCR assays to investigate the enrichment of TaVrt2 and TaVrn1 at the *TaVrn1* locus using

overexpression lines carrying p*UBI-TaVrt2-YFP* and p*UBI-TaVrn1-YFP*, respectively. The distributions of TaVrn1 and TaVrt2 were investigated at five sites in the promoter and the first intron of *TaVrn1* **(Fig. 6A)**. The ChIP-qPCR assays showed that TaVrt2 was significantly enriched at the two sites around the CArG box in the *TaVrn1* promoter, indicating that TaVrt2 can bind to the *TaVrn1* promoter **(Fig. 6B)**. However, no significant enrichment of TaVrn1 was detected at any target site, showing that TaVrn1 proteins cannot or only weakly bind to the promoter of *TaVrn1* **(Fig. 6B)**.

The above results suggested that *TaVrn1-5DL* (the dominant *TaVrn1* allele in KN199, the transgenic recipient cultivar) showed the largest upregulation in *TaVrt2*-OE and *TaVrn1*-OE compared with *TaVrn1-5AL* and *TaVrn1-5BL* (the recessive *TaVrn1* alleles) **(Fig. 5B and 5C)**. In order to compare the binding of TaVrt2 and TaVrn1 to *TaVrn1-5AL*, *TaVrn1-5BL* and *TaVrn1-5DL* promoter, a genome-specific amplification primer across CArG box on *TaVrn1* promoter was designed to investigate the distributions of TaVrn1 and TaVrt2 (shown by a purple line across CArG box in **Fig. 6A**). ChIP-qPCR showed that TaVrn1 had no significant enrichment on the promoters of *TaVrn1* orthologues, consistent with the results above **(Fig. 6B and 6C)**. In contrast, TaVrt2 had significant enrichment on promoters of *TaVrn1-5AL* and *TaVrn1-5DL*, but insignificantly enriched on *TaVrn1-5BL* promoter. In addition, TaVrt2 on *TaVrn1-5DL* promoter had higher enrichment than that on *TaVrn1-5AL* and *TaVrn1-5BL*. The binding ability of TaVrt2 at CArG box of *TaVrn1* looks significant correlation with their expression activity (**Fig. 5B, 5C and 6C**).

TaVrt2 and *TaVrn1* are subject to different chromatin remodeling responses to vernalization

It is reported that vernalization up-regulates *TaVrn1* expression through dynamic changes of H3K4me3 and H3K27me3 at the *TaVrn1* locus (Oliver et al., 2009; Diallo et al., 2012). Since *TaVrt2* is induced by vernalization just as *TaVrn1*, we compared the level of H3K4me3 and H3K27me3 modification at the *TaVrt2* and *TaVrn1* loci in vernalization or non-vernalization conditions, to find out whether they undergo similar epigenetic regulation. We confirmed that H3K27me3 decreased at *TaVrn1* locus on 25th day of vernalization (V25) compared to non-vernalization condition (N25) **(Fig. 7A and 7B)**. However, H3K4me3 at *TaVrn1* had no significant enrichment change between V0 and V25 conditions. Additionally, we had not detected significant difference of H3K4me3 and H3K27me3 modification at the *TaVrt2* locus between V25 and N25 conditions (**Fig. 7C and 7D**). Thus, although both *TaVrt2* and *TaVrn1* are induced by

vernalization, their responses to vernalization may be regulated by different epigenetic regulatory machineries.

Discussion

SVP-like genes underwent functional differentiation for vernalization-mediated flowering

TaVrt2 was previously reported to be repressed by vernalization and inhibited the expression of *TaVrn1*, a flowering promoter in the vernalization pathway (Kane et al., 2005; Kane et al., 2007). Consequently, *TaVrt2* was regarded as a flowering repressor in the vernalization pathway. However, later studies suggested that *TaVrt2* and *HvVrt2* were induced by vernalization, contradictory to the earlier reports (Trevaskis et al., 2007; Dubcovsky et al., 2008; Winfield et al., 2009; Li et al., 2017). In this study, we investigated the transcriptional pattern of *TaVrt2* and found that it was strongly induced by vernalization **(Fig. 3C)**. Transgenic experiments showed that lines overexpressing *TaVrt2* flowered earlier than NC under non- or incomplete vernalization conditions **(Fig. 1)**, indicating that *TaVrt2* is a flowering promoter in the vernalization-regulated pathway.

TaVrt2 has the highest similarity to *SVP* in the model eudicot *Arabidopsis* (Kane et al., 2005). *SVP* was reported as a flowering inhibitor in *Arabidopsis* and vernalization has little effect on its expression (Hartmann et al., 2000; Li et al., 2008; Kim et al., 2009). Obviously, *SVP* genes are subject to functional differentiation in response to vernalization between *Arabidopsis* and wheat. Moreover, SVP represses vernalization-mediated flowering via interaction with the core component FLC in *Arabidopsis* (Li et al., 2008). Here we validated that TaVrt2 promoted flowering in wheat by interplay with the central regulator of vernalization, TaVrn1. Our findings not only increases understanding of the vernalization-regulated flowering pathway in temperate grasses but also sheds further light on the distinctive vernalization mechanisms in the *Triticeae* and *Brassicaceae*, represented by wheat and *Arabidopsis*, respectively.

In addition to the functional diversification between different species, *SVP*-like genes evolved into multiple paralogues in each species. The phylogenetic tree showed that each grass species, such as wheat, barley, *Brachypodium*, rice and maize, contains three *SVP*-like genes belonging to different clusters **(Fig. S2A)**, indicating that these *SVP* paralogues were generated prior to the divergence of *Poaceae*. However, the *Poaceae* primarily consists of tropical species and vernalization was only required for temperate cereals (e.g., wheat, barley and *Brachypodium*) and not for other grass

species, such as maize and rice (Zhong et al., 2018). Therefore, we speculate that the original function of *SVP*-like genes is irrelevant to vernalization and their vernalization-regulated function is gained evolutionarily under low temperature stress. In other words, *SVP* may be an important domestication gene and its functional variation can be instrumental in promoting plants to adapt local environments.

TaVrt2, *WM22* and *WM28* are *SVP*-like genes in wheat and their barley orthologues are *HvVrt2*, *BM10* and *BM1*, respectively. Although *BM1* and *BM10* are induced by vernalization, RNAi of *BM1* and *BM10* did not change heading date in barley, suggesting that *BM1* and *BM10* are not involved in regulation of flowering time (Trevaskis et al., 2007). However, the *BM1*-OE delayed heading date by approximately 10 d, whereas *BM10* OE had no effect on head emergence (Trevaskis et al., 2007). *HvVrt2* is also induced by vernalization, but its function in flowering time remains unknown. Here we investigated the expression of *TaVrt2*, *WM22* and *WM28* in wheat **(Fig. S2B)**. Although all of them were induced by vernalization, *TaVrt2* had the highest expression level under vernalization conditions. In terms of response to vernalization, *TaVrt2* is more important in regulation of vernalization than *WM22* and *WM28*. However, it is still possible that *WM22* and *WM28* have abundant function with *TaVrt2* because they are expressed in leaves and are slightly induced by vernalization. In our previous Y2H assays, WM22 also bound with TaVrn1 in a similar way to TaVrt2 (Cao and Yan, 2013). Therefore, it is necessary to determine the functions of *WM22* and *WM28* and to pinpoint their genetic relationship with *TaVrt2* and *TaVrn1* in the wheat vernalization-regulated flowering pathway by transgenic experiments.

TaVrt2 probably acts as a fine-tuner for vernalization-mediated flowering

In this study, overexpression of *TaVrt2* promoted flowering only by an average 6.2 and 5.4 d relative to NC under non- and incomplete vernalization, respectively (**Fig.1**). In contrast, overexpression of some other flowering genes, such as *TaVrn3* and *TaVer2*, in the vernalization pathway, advanced flowering by more than 40 d than the respective NC (Lv et al., 2014; Xiao et al., 2014). *TaVrt2* was strongly induced during vernalization but its levels sharply declined after vernalization, indicating that *TaVrt2* mainly functions during vernalization and has little effect on flowering after vernalization (**Fig. 3**). TaVrt2 can promote *TaVrn1* expression and directly binds with its promoter, suggesting that the effect of TaVrt2 on flowering may be mediated by TaVrn1 (**Fig. 5 and 6**). It is therefore assumed that TaVrt2 functions as a co-factor to initiate auto-activation of *TaVrn1*. Since *TaVrn1* is the core gene in the vernalization regulatory pathway, the

function of *TaVrt2* in regulating vernalization-mediated flowering probably depends to great extent on the expression of *TaVrn1*. Taken together, *TaVrt2* may function as a co-factor of *TaVrn1* in fine-tuning flowering in the vernalization pathway.

TaVrt2 mediates a positive feedback loop of _TaVrn1_ self-regulation in the vernalization flowering pathway

Many studies showed that the MADS-box TF usually regulates its downstream target genes through formation of homo- or heter-dimers (de Folter et al., 2005; Kaufmann et al., 2005). The core regulator *TaVrn1* in the wheat vernalization flowering pathway encodes a MADS-box TF. Previous studies showed that TaVrn1 could bind with another MADS-box TF, TaVrt2 (Kane et al., 2005; Cao and Yan, 2013). Here, we confirmed that TaVrt2 and TaVrn1 could interact with each other *in vitro*, *in planta* and in wheat cells through pull-down (**Fig. 2A**), luciferase complementation imaging (**Fig. 2B**) and BiFC (**Fig. 2C**) assays; both of them can also be induced by vernalization in leaves (**Fig. 3A, 3B and 3C**). Wheat transgenic assays showed that both *TaVrt2* and *TaVrn1* were flowering promoters in the vernalization pathway (**Fig. 1 and S3**). Transcriptomic analyses further revealed that both *TaVrt2* and *TaVrn1* could significantly upregulate *TaVrn1*. Previous studies showed that TaVrt2 could bind with the CArG-box in the *TaVrn-1* promoter *in vitro* (Kane et al., 2007; Dubcovsky et al., 2008). Our ChIP-qPCR assays displayed that TaVrt2 directly interacted with the *TaVrn1* promoter *in vivo*. However, we did not detect significant accumulation of TaVrn1 at the corresponding sites. These results indicated that TaVrn1 might achieve self-regulation through interaction with TaVrt2.

We proposed a positive feedback loop to exhibit the cooperative regulatory mechanism underlying TaVrt2 and TaVrn1 in the vernalization flowering pathway in winter wheat **(Fig. 8)**. According to the model, after germination in the fall, *TaVrt2* and *TaVrn1* in winter wheat are expressed at very low levels prior to vernalization, and cannot form a sufficient regulatory complex to promote expression of *TaVrn1*. *TaVrt2* and *TaVrn1* are gradually upregulated during cold winter temperatures, and the complex massively accumulates and binds with the CArG box in the *TaVrn1* promoter. As a result, *TaVrn1* moderately increases at the beginning of vernalization and later undergoes a rapid increase. With rising temperatures in spring, *TaVrt2* expression sharply declines and quite few regulatory complexes are available to accelerate the expression of *TaVrn1*. Consequently, *TaVrn1* expression undergoes a concomitant short reduction after vernalization. Subsequently, *TaVrn1* again increases, indicating regulation by other factors. *TaVrn3* (*TaFT*)

expression is regulated by *TaVrn1*, and the TaVrn3/TaFDL2 complex has also been reported to upregulate *TaVrn1* (Li and Dubcovsky, 2008; Chen and Dubcovsky, 2012; Deng et al., 2015). Additionally, transcriptional pattern assays showed that the expression of *TaVrn3* was very low during vernalization and increased greatly after vernalization, while *TaFDL2* expressed constitutively, suggesting that their encoded proteins would be available to interact each other after vernalization **(Fig. S5)**. When *TaVrn1* expression reaches to a certain threshold, it activates *TaVrn3* expression, and *TaVrn1* is further activated by the TaVrn3/TaFDL2 complex (Li and Dubcovsky, 2008). As such, we assume that during vernalization, *TaVrn1* is mainly activated by a TaVrt2-mediated positive self-regulatory loop, and after vernalization, primarily modulated through the TaVrn3/TaFDL2 complex-mediated positive feedback loop **(Fig. 8)**.

Acknowledgments

We thank Prof. Jiaqiang Sun (Institute of Crop Sciences, CAAS) for supplying the pCAMBIA1300cLUC and pCAMBIA1300nLUC vectors and technical assistance for the LCI assay. We also thank Prof. Robert McIntosh (Plant Breeding Institute, University of Sydney), Prof. Takato Imaizumi (University of Washington) and Prof. Andrew Doust for review and suggestions regarding the manuscript. This study was funded by National Natural Science Foundation of China (91935304 and 3151663), National Key R&D program of China (2016ZX08009003 and 2016YFD0100502) and CAAS Science and Technology Innovation Program.

Author contributions

LX, XL, DX, XT and LL performed the experiments; KW and XY conducted the genetic transformations of wheat; SC designed the project; LX and SC wrote the draft; SC, YZ, XX, WL and LY revised the paper.

References

Cao S, Yan L. 2013. Construction of a high-quality yeast two-hybrid (Y2H) library and its application in identification of interacting proteins with key vernalization regulator TaVRN-A1 in wheat. *BMC Research Notes* **6:** 81.

Cao S, Kumimoto RW, Siriwardana CL, Risinger JR, Holt BF 3rd. 2011. Identification and characterization of *NF-Y* transcription factor families in the monocot model plant *Brachypodium distachyon*. *PLoS One* **6:** e21805.

Chen A, Dubcovsky J. 2012. Wheat TILLING mutants show that the vernalization gene *VRN1* down-regulates the flowering repressor *VRN2* in leaves but is not essential for flowering. *PLoS Genetics* **8:** e1003134.

de Folter S, Immink RG, Kieffer M, Parenicova L, Henz SR, Weigel D, Busscher M, Kooiker M, Colombo L, Kater MM et al. 2005. Comprehensive interaction map of the *Arabidopsis* MADS box transcription factors. *Plant Cell* **17:** 1424-1433.

Deng W, Casao MC, Wang P, Sato K, Hayes PM, Finnegan EJ, Trevaskis B. 2015. Direct links between the vernalization response and other key traits of cereal crops. *Nature Communication* **6:** 5882.

Danyluk J, Kane NA, Breton, G, Limin, AE, Fowler, DB, Sarhan, F. 2003. *TaVRT-1*, a putative transcription factor associated with vegetative to reproductive transition in cereals. *Plant Physiology* **132:** 1849-1860.

Diallo AO, Ali-Benali MA, Badawi M, Houde M, Sarhan F. 2012. Expression of vernalization responsive genes in wheat is associated with histone H3 trimethylation. *Molecular Genetics and Genomics* **287:** 575-590.

Distelfeld A, Li C, Dubcovsky J. 2009. Regulation of flowering in temperate cereals. *Current Opinion in Plant Biology* **12:** 178-184.

Dubcovsky J, Li C, Distelfeld A, Pidal B, Tranquilli G. 2008. Genes and gene networks regulating wheat development. *In*: Appels R, Eastwood R, Lagudah E, Langridge P, Mackay M, McIntyre L, Sharp P, (Eds.). Proceedings of 11th International Wheat Genetics Symposium. Sydney University Press. 25-29 August 2008, Brisbane, Australia.

Ferrari K, Scelfo A, Jammula S, Jammula S, Cuomo A, Barozzi I, Stutzer A, Fischle W,

Bonaldi T, Pasini D. 2014. Polycomb-dependent H3K27me1 and H3K27me2 regulate active transcription and enhancer fidelity. *Molecular Cell* **53:** 49-62.

Fu D, Szucs P, Yan L, Helguera M, Skinner JS, von Zitzewitz J, Hayes PM, Dubcovsky J. 2005. Large deletions within the first intron in *VRN-1* are associated with spring growth habit in barley and wheat. *Molecular Genetics and Genomics* **273**: 54-65.

Hartmann U, Hohmann S, Nettesheim K, Wisman E, Saedler H, Huijser P. 2000. Molecular cloning of *SVP*: a negative regulator of the floral transition in *Arabidopsis*. *Plant Journal* **21:** 351-360.

Ishida Y, Tsunashima M, Hiei Y, Komari T. 2015. Wheat (*Triticum aestivum* L.) transformation using immature embryos. *Methods in Molecular Biology* **1223**: 189-198.

Kane NA, Agharbaoui Z, Diallo AO, Adam H, Tominaga Y, Ouellet F, Sarhan F. 2007. TaVRT2 represses transcription of the wheat vernalization gene *TaVRN1*. *Plant Journal* **51:** 670-680.

Kane NA, Danyluk J, Tardif G, Ouellet F, Laliberte JF, Limin AE, Fowler DB, and Sarhan F. 2005. *TaVRT-2*, a member of the *StMADS-11* clade of flowering repressors, is regulated by vernalization and photoperiod in wheat. *Plant Physiology* **138:** 2354-2363.

Kaufmann K, Melzer R, Theissen G. 2005. MIKC-type MADS-domain proteins: structural modularity, protein interactions and network evolution in land plants. *Gene* **347:** 183-198.

Kim DH, Doyle MR, Sung S, Amasino RM. 2009. Vernalization: winter and the timing of flowering in plants. *Annual Review of Cell and Developmental Biology* **25:** 277-299.

Kippes N, Debernardi JM, Vasquez-Gross HA, Akpinar BA, Budak H, Kato K, Chao S, Akhunov E, and Dubcovsky J. 2015. Identification of the *VERNALIZATION 4* gene reveals the origin of spring growth habit in ancient wheats from South Asia. *Proceedings of the National Academy of Sciences, USA* **112:** 5401-5410.

Li C, Dubcovsky J. 2008. Wheat FT protein regulates *VRN1* transcription through interactions with FDL2. *Plant Journal* **55:** 543-554.

Li C, Distelfeld A, Comis A, Dubcovsky J. 2011. Wheat flowering repressor VRN2 and promoter CO2 compete for interactions with NUCLEAR FACTOR-Y complexes. *Plant Journal* **67:** 763-773.

Li D, Liu C, Shen L, Wu Y, Chen H, Robertson M, Helliwell CA, Ito T, Meyerowitz E, Yu H. 2008. A repressor complex governs the integration of flowering signals in *Arabidopsis*. *Developmental Cell* **15:** 110-120.

Li Q, Byrns B, Badawi M.Y, Diallo AB, Danyluk J, Sarhan F, Laudencia-Chingcuanco D, Zou J, Fowler DB. 2017. Transcriptomic insights into phenological development and cold tolerance of wheat grown in the field. *Plant Physiology* **176:** 2376-2394.

Luo C, Lam E. 2014. Quantitatively profiling genome-wide patterns of histone modifications in *Arabidopsis thaliana* using ChIP-seq. *Methods in Molecular Biology* **1112,** 177-193.

Lv B, Nitcher R, Han X, Wang S, Ni F, Li K, Pearce S, Wu J, Dubcovsky J, Fu D. 2014. Characterization of *FLOWERING LOCUS T1* (*FT1*) gene in *Brachypodium* and wheat. *PloS One* **9:** e94171.

Mandel MA., Gustafson-Brown C, Savidge B, Yanofsky MF. **1992.** Molecular characterization of the *Arabidopsis* floral homeotic gene *APETALA1*. *Nature* **360**: 273-277.

Milec Z, Valarik M, Bartos J, Safar J. 2014. Can a late bloomer become an early bird? Tools for flowering time adjustment. *Biotechnology Advances* **32:** 200-214.

Mo Y, Vanzetti LS, Hale I, Spagnolo EJ, Guidobaldi F, Al-Oboudi J, Odle N, Pearce S, Helguera M, Dubcovsky J. 2018. Identification and characterization of *Rht25*, a locus on chromosome arm 6AS affecting wheat plant height, heading time, and spike development. *Theoretical and Applied Genetics* **131**: 2021-2035.

Oliver SN, Finnegan EJ, Dennis ES, Peacock WJ, Trevaskis B. 2009. Vernalization-induced flowering in cereals is associated with changes in histone methylation at the *VERNALIZATION1* gene. *Proceedings of the National Academy of Sciences, USA* **106:** 8386-8391.

Schmittgen TD, Livak KJ. 2008. Analyzing real-time PCR data by the comparative CT method. *Nature Protocols* **3:** 1101-1108.

Shan Q, Wang Y, Li J, Gao C. 2014. Genome editing in rice and wheat using the CRISPR/Cas system. *Nature Protocols* **9:** 2395-2410.

Sun J, Qi L, Li Y, Zhai Q, Li C. 2013. PIF4 and PIF5 transcription factors link blue light and auxin to regulate the phototropic response in *Arabidopsis*. *Plant Cell* **25:** 2102-2114.

Trevaskis B, Bagnall DJ, Ellis MH, Peacock WJ, Dennis ES. 2003. MADS box genes control vernalization-induced flowering in cereals. *Proceedings of the National Academy of Sciences, USA* **100:** 13099-13104.

Trevaskis B, Tadege M, Hemming MN, Peacock WJ, Dennis ES, Sheldon C. 2007. *Short vegetative phase*-like MADS-box genes inhibit floral meristem identity in barley. *Plant Physiology* **143:** 225-235.

Waadt R, Schmidt LK, Lohse M, Hashimoto K, Bock R, Kudla J. 2008. Multicolor bimolecular fluorescence complementation reveals simultaneous formation of alternative CBL/CIPK complexes *in planta*. *Plant Journal* **56:** 505-516.

Winfield MO, Lu C, Wilson ID, Coghill JA, and Edwards KJ. 2009. Cold- and light-induced changes in the transcriptome of wheat leading to phase transition from vegetative to reproductive growth. *BMC Plant Biology* **9**: 55.

Xiao J, Xu S, Li C, Xu Y, Xing L, Niu Y, Huan Q, Tang Y, Zhao C, Wagner D et al. 2014. O-GlcNAc-mediated interaction between VER2 and TaGRP2 elicits *TaVRN1* mRNA accumulation during vernalization in winter wheat. *Nature Communication* **5:** 4572.

Xu S, Chong K. 2018. Remembering winter through vernalisation. *Nature Plants* **4:** 997-1009.

Yan L, Loukoianov A, Tranquilli G, Helguera M, Fahima T, Dubcovsky J. 2003. Positional cloning of the wheat vernalization gene *VRN1*. *Proceedings of the National Academy of Sciences, USA* **100:** 6263-6268.

Yan L, Loukoianov A, Blechl A, Tranquilli G, Ramakrishna W, SanMiguel P, Bennetzen JL, Echenique V, Dubcovsky J. 2004a. The wheat *VRN2* gene is a flowering repressor down-regulated by vernalization. *Science* **303:** 1640-1644.

Yan L, Helguera M, Kato K, Fukuyama S, Sherman J, Dubcovsky J. **2004b.** Allelic variation at the *VRN-1* promoter region in polyploid wheat. *Theoretical and Applied Genetics* **109**: 1677-1686.

Yan L, Fu D, Li C, Blechl A, Tranquilli G, Bonafede M, Sanchez A, Valarik M, Yasuda S, Dubcovsky J. 2006. The wheat and barley vernalization gene *VRN3* is an orthologue of *FT*. *Proceedings of the National Academy of Sciences, USA* **103:** 19581-19586.

Zhang XK, Xiao YG, Zhang Y, Xia XC, Dubcovsky J, He ZH. 2008. Allelic variation at the

vernalization genes *Vrn-A1*, *Vrn-B1*, *Vrn-D1*, and *Vrn-B3* in Chinese wheat cultivars and their association with growth habit. *Crop Science* **48**: 458-470.

Zhong J, Robbett M, Poire A, Preston JC. 2018. Successive evolutionary steps drove *Pooideae* grasses from tropical to temperate regions. *New Phytologist* **217:** 925-938.

Figure legends

Fig. 1 Functional validation of *TaVrt2* in the wheat vernalization flowering pathway

A, C and E show statistical analyses of flowering time in *TaVrt2* overexpression (OE) lines and negative controls (NC) including KN199 and transgenic null lines (TNL) under 0-day (A), 10-day (C) and 30-day (E) vernalization conditions, respectively. TNL were a composite of *TaVrt2*-L23(-), *TaVrt2*-L30(-) and *TaVrt2*-L35(-). Asterisks above bars indicate statistically significant differences between transgenic lines and both KN199 and TNL at **P*<0.05, ***P*<0.01 and ****P*<0.001. NS: not significant. The flowering date and error bar represent the average and SD from 10 plants. B, D and F show the phenotypes of *TaVrt2*-OE and TNL under 0-day (B), 10-day (D) and 30-day (F) vernalization conditions, respectively. *TaVrt2*-L35(+) and *TaVrt2*-L35(-) lines were used as representative lines for *TaVrt2* overexpression and TNL, respectively. Both *TaVrt2*-L35(+) and *TaVrt2*-L35(-) were the offspring from *TaVrt2*-L35. Scale bar, 30 cm.

Fig. 2 Validation of physical interaction between wheat TaVrt2 and TaVrn1 through multiple approaches

A. *In vitro* pulldown assays to verify TaVrt2 binding with TaVrn1. GST and MBP were used as negative controls. The solid red and blue arrows indicate TaVrt2-GST and GST proteins, respectively, whereas the hollow red and blue arrows indicate TaVrn1-MBP and MBP proteins, respectively. B. LCI analyses to demonstrate the interaction between TaVrt2 and TaVrn1 in *Nicotiana benthamiana* leaves. TaVrt2-cLUC/nLUC, TaVrn1-nLUC/cLUC and nLUC/cLUC were used as negative controls. Compared to the negative controls, the positive signal was detected in the TaVrt2-cLUC/TaVrn1-nLUC co-transformed area in *Nicotiana benthamiana* leaf. C. BiFC assays in wheat protoplasts for TaVrt2 and TaVrn1 interaction. TaVrt2-cYFP/nYFP and TaVrn1-nYFP/cYFP were used as negative controls. Scale bar, 50 μm. Compared to the negative controls, the positive signal was detected in the TaVrt2-cYFP/TaVrn1-nYFP co-transformed wheat protoplast.

Fig. 3 Spatio-temporal expression patterns of *TaVrt2* and *TaVrn1* in wheat

A. Expression of *TaVrt2* and *TaVrn1* in different tissues. Leaves and roots were harvested during vernalization. Stems and spikes (young) were sampled at the booting stage. Florets and grains (immature) were collected at flowering and 7 days (d) after pollination, respectively. B. Schematic for treatments and sampling time-points. Three-week old plants grown in normal temperatures were exposed to cold temperature (2-4°C and 16 h light/8h darkness) for 35 d and then recovered in the normal temperature (15-18°C and 16 h light/8h darkness). Sampling time-points indicated

by arrows include no vernalization (V0), vernalization for 7 d (V7), 21 d (V21), 35 d (V35), recovery for 7 d (V35N7) and 21 d (V35N21) under normal growing conditions (15-18°C and 16 h light/8h darkness) after 35-day vernalization. Blue and green colors indicate cold and normal growth conditions, respectively. C. Response of *TaVrt2* and *TaVrn1* to vernalization. Three cultivars including Kenong199 (KN199, weak winter type), Jimai22 (semi-winter type), Zhongmai175 (strong winter type) were used to investigate the transcriptional patterns of *TaVrt2* and *TaVrn1*. A photoperiod of 16 h light / 8 h darkness was used during vernalization. Orange and blue curves indicate the transcriptional patterns of *TaVrt2* or *TaVrn1* under vernalization and none-vernalization treatments, respectively. Bar represents the standard deviation of three biological replications at each time point.

Fig. 4 The genetic interaction between wheat *TaVrn1* and *TaVrt2*

A. Relative expression of *TaVrt2* and *TaVrn1* in the negative control (NC, i.e. transgenic null lines), *TaVrn1*-OE lines (1: H-*TaVrn1*), *TaVrt2*-OE lines (2: H-*TaVrt2*) and double OE lines (3: H-*TaVrt2*+*TaVrn1*) identified from the F_2 population of a cross between *TaVrt2*-OE and *TaVrn1*-OE lines. Bars represent the standard deviations of three biological replications at each time point. The conserved primer pair was used to investigate the overall expression level of transgenic and native target gene. B. Two-way interaction analyses between *TaVrn1* and *TaVrt2* for flowering time after a 10-day vernalization period (incomplete vernalization). Left panel shows flowering time and significant difference in NC, H-*TaVrt2*, H-*TaVrn1* and H-*TaVrt2*+*TaVrn1*. **P*<0.05, ***P*<0.01 and ****P*<0.001. The right panel indicates the significance test of *TaVrt2*, *TaVrn1* and *TaVrt2*×*TaVrn1* effects on flowering time. Proc GLM (SAS 9.04) was used to estimate the *P* value. C. Phenotype of NC, H-*TaVrn1*, H-*TaVrt2* and H-*TaVrn1*+*TaVrt2* under incomplete vernalization conditions. Scale bar, 30 cm. 1-3 are the same wheat lines as in A.

Fig. 5 Common targets regulated by wheat *TaVrt2* and *TaVrn1*

A. Differential expression analysis of genes in *TaVrt2*-OE and *TaVrn1*-OE lines based on RNA-seq. The overlapping part of the orange and blue cycles indicates the number of differentially expressed genes shared by *TaVrt2*-OE and *TaVrn1*-OE lines compared to transgenic null lines (TNL). B and C showed relative expression of *TaVrn1-5DL* and *TaVrn1-5AL*, respectively, in TNL, *TaVrt2*-OE and *TaVrn1*-OE lines based on qPCR. The primers specific to *TaVrn1* were used to investigate the expression level of their native versions. The growth conditions of plants and sampling timepoints were the same as those in RNA-seq assays. Fresh leaves from five individuals in each line were collected on the 15th day after the 10-day vernalization period. NS: not

significant; *P<0.05, **P<0.01 and ***P<0.001. The error bars represent SD (standard deviation). D. Relative expression of *TaVrn1-5DL* in NC, H-*TaVrt2*, H-*TaVrn1* and H-*TaVrt2*+*TaVrn1* at different developmental stages. V0, V10 and V10N5 indicate no vernalization, 10-day vernalization and recovery for 5 days after the 10-day vernalization period. NC, H-*TaVrt2*, H-*TaVrn1* and H-*TaVrt2*+*TaVrn1* represent TNL, *TaVrt2*-OE, *TaVrn1*-OE and double OE lines, respectively. *P<0.05, **P<0.01 and ***P<0.001. The error bars represent SD.

Fig. 6 Relative enrichment distribution of TaVrt2 and TaVrn1 at *TaVrn1* locus in wheat

A. Scaled diagram of the *TaVrn1* locus showing sites for ChIP-qPCR. CArG box is the potential TaVrt2 binding site. TSS (transcription start site) and exon 1 of *TaVrn1* are labeled. B. Relative enrichment (fold) of TaVrt2 and TaVrn1 in the *TaVrn1* loci (including *TaVrn1-5AL*, *TaVrn1-5BL* and *TaVrn1-5DL*) based on ChIP-qPCR assays. 1-5 show the investigated sites as in A. *P<0.05, **P<0.01 and ***P<0.001; the error bars represent SD (standard deviation). TNL: transgenic null lines. C. Relative enrichment (fold) of TaVrt2 and TaVrn1 in the CArG box regions of *TaVrn1-5AL*, *TaVrn1-5BL* and *TaVrn1-5DL* promoter, respectively. The genome-specific site is shown by the purple line across CArG box in A. *P<0.05, **P<0.01 and ***P<0.001; the error bars represent SD.

Fig. 7 The effect of vernalization on H3K4me3 and H3K27me3 distribution at the *TaVrn1* and *TaVrt2* loci in wheat

Diagram of the *TaVrn1* (A) and *TaVrt2* (C) loci showing the sites (1-6 shown by short black lines) for ChIP-qPCR. The vertical black line indicates the transcription start site (TSS) and the vertical rectangles indicate exons. Relative enrichment of H3K4me3 and H3K27me3 at the *TaVrn1* (B) and *TaVrt2* (D) loci were compared in vernalization or non-vernalization treatments. Each value represents the mean of three biological experiments with ± SD and was normalized to the non-vernalization level in each site. *P<0.05, **P<0.01 and ***P<0.001; the error bars represent SD (standard deviation).

Fig. 8 A proposed model for positive feedback regulation of *TaVrn1* mediated by the TaVrt2-TaVrn1 and TaVrn3-TaFTL2 complexes in the wheat vernalization flowering pathway.

The upper panel is a schematic of the expression patterns of *TaVrt2*, *TaVrn1*, *TaVrn3* and *TaFDL2* before, during and after vernalization. Their expression patterns based on qPCR assays are shown in **Fig. 3** or **Fig. S5**. The high and low abundance of TaVrn3 (purple), TaFDL2 (green), TaVrn1 (red) and TaVrt2 (blue) proteins is shown in dark and light colors, respectively. G- and CArG- represent the G box and CArG box, the binding sites of TaFDL2 and TaVrt2, respectively, on the

TaVrn1 promoter. TSS: transcription start site. The black arrows with dashed, thin and bold lines indicate little, weak and strong transcription levels of *TaVrn1,* respectively. Blue and green curves with arrows indicate the feedback of *TaVrn1* expression to TaVrn1 and TaVrn3 proteins, respectively.

Supporting information

Fig. S1 Relative expression of *TaVrt2* in wheat transgenic lines

Fig. S2 Evolutionary differentiation and functional variation of *SVP*-like genes

Fig. S3 Phenotype of wheat *TaVrn1* OE lines

Fig. S4 Genotyping of vernalization genes *TaVrn1* and *TaVrn3* in wheat cultivar KN199

Fig. S5 Expression patterns of *TaVrt2*, *TaVrn1*, *TaVrn3* and *TaFDL2* in wheat cultivar KN199 before, during and after vernalization

Table S1 List of primers used in this study

Table S2 Primer pairs and expected band sizes for different alleles at the *TaVrn1* and *TaVrn3* loci

Dataset S1 Identification of the comment targets of TaVrt2 and TaVrn1 using RNA-seq assays

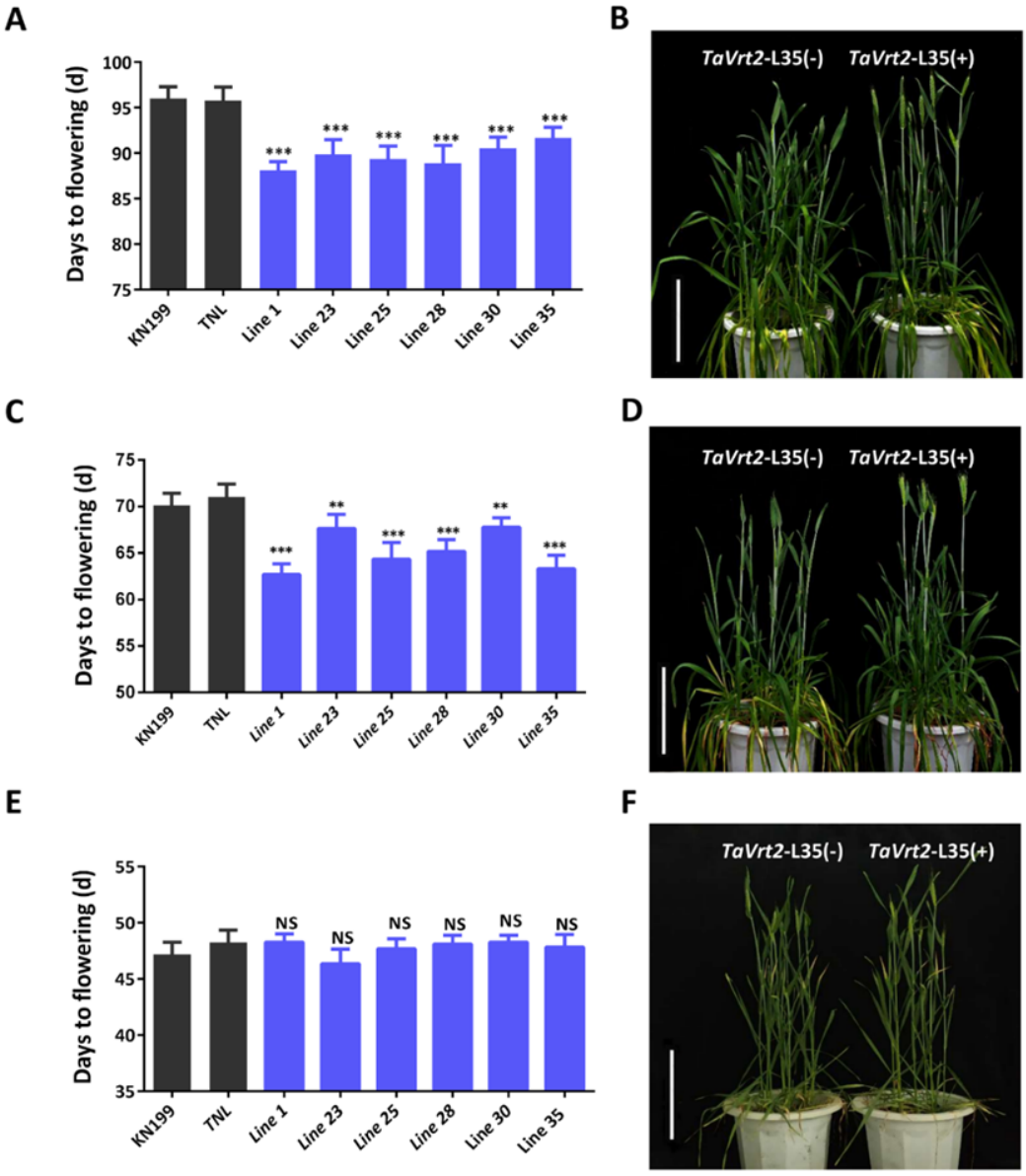

nph_16339_f1.png

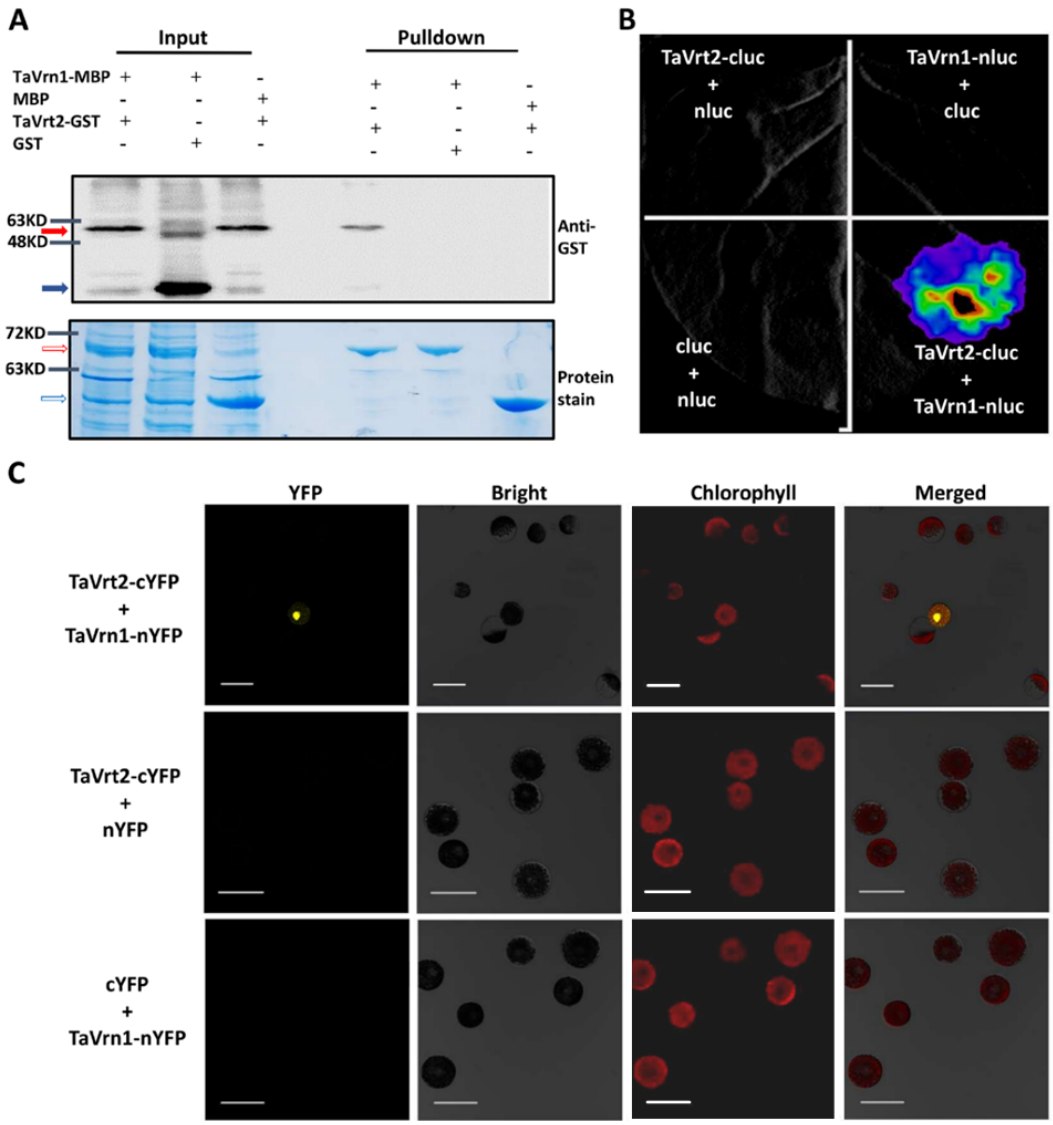

nph_16339_f2.png

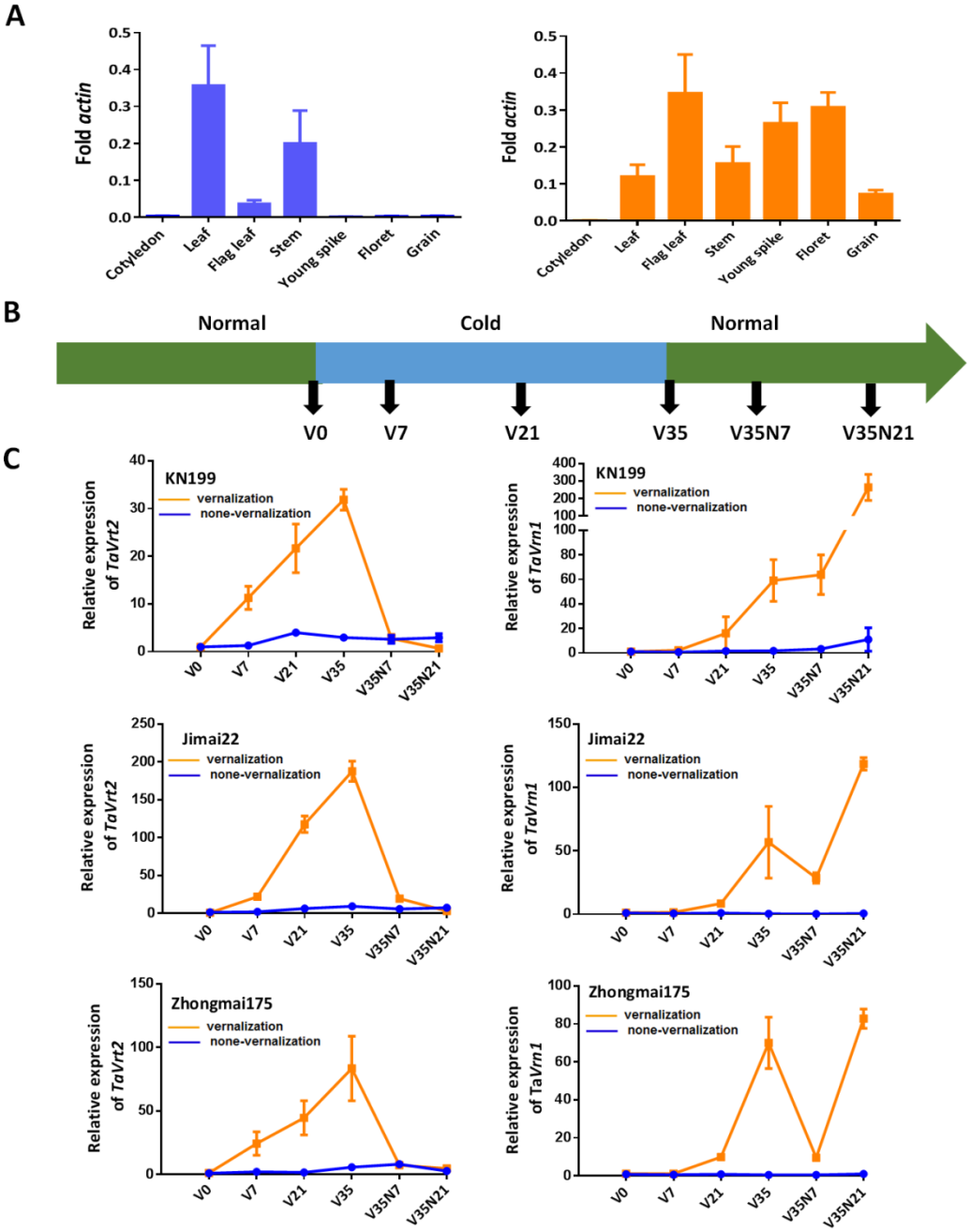

nph_16339_f3.png

A

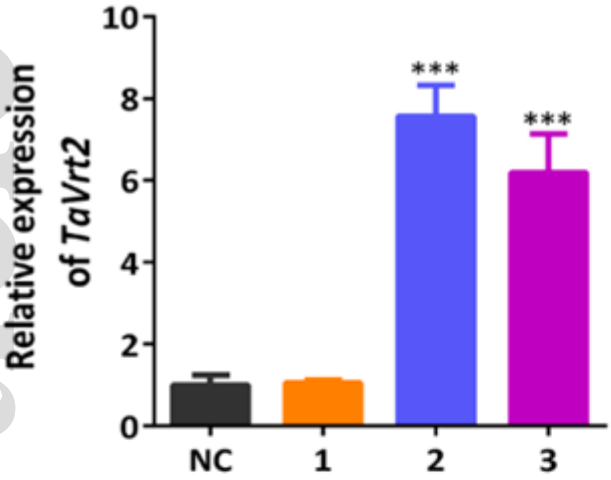

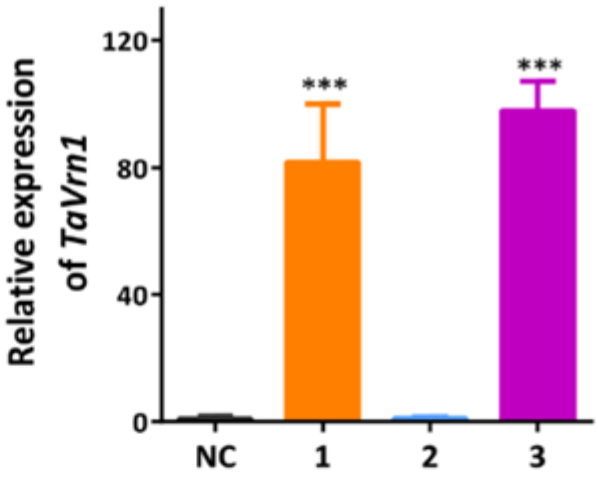

B

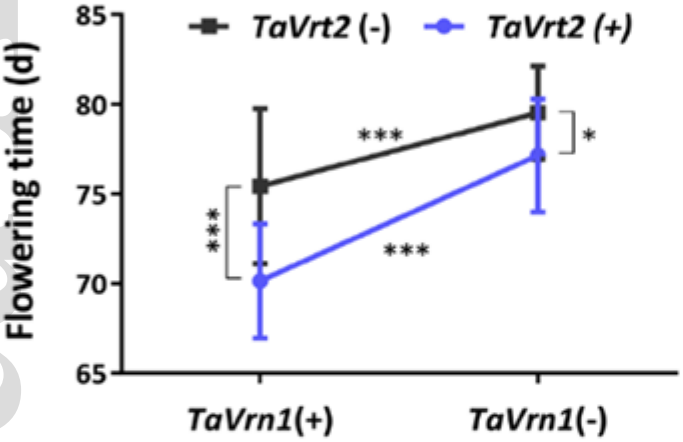

Effect	P value
TaVrt2	<0.001
TaVrn1	<0.001
TaVrt2 X *TaVrn1*	<0.05

C

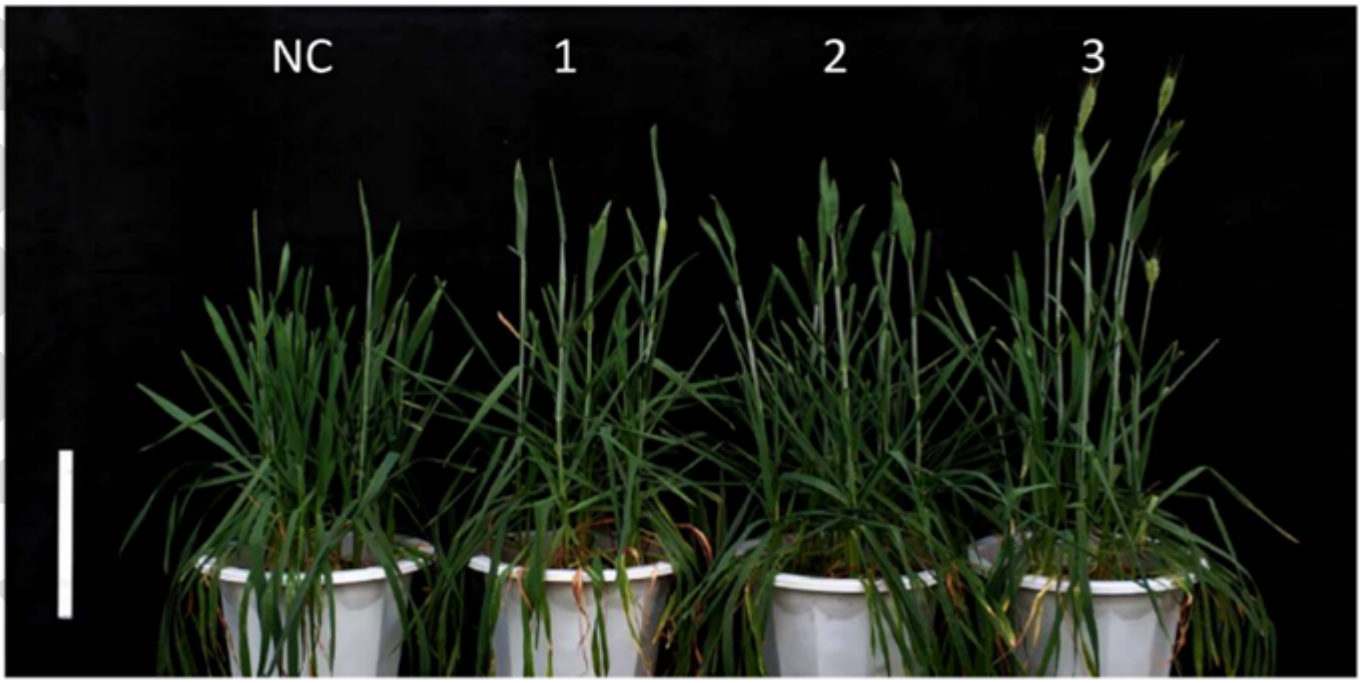

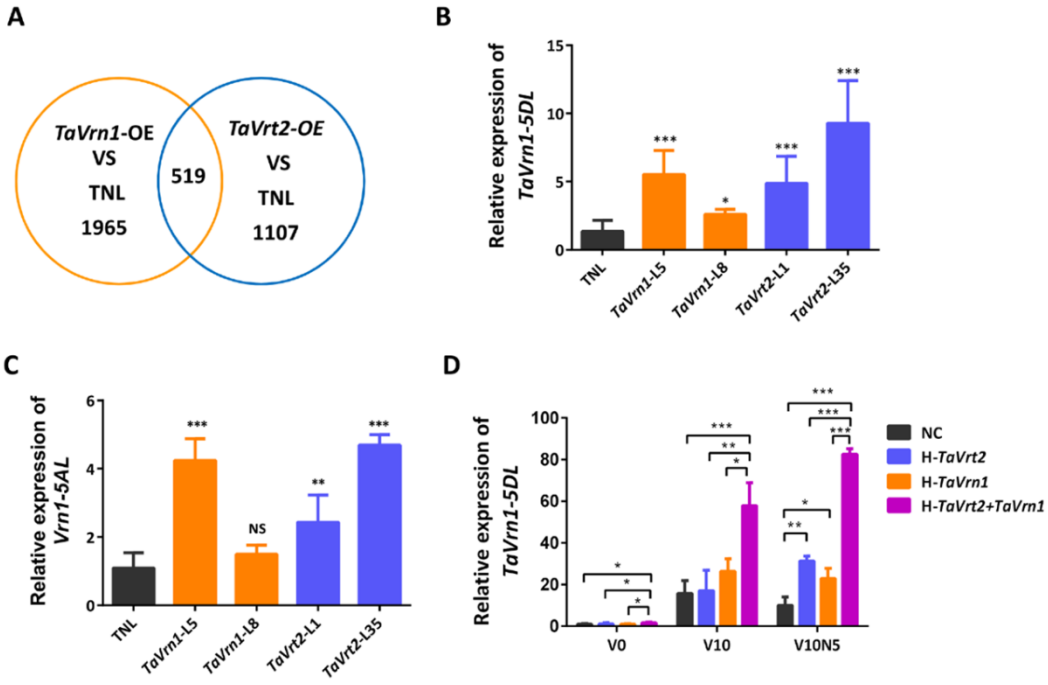

nph_16339_f5.png

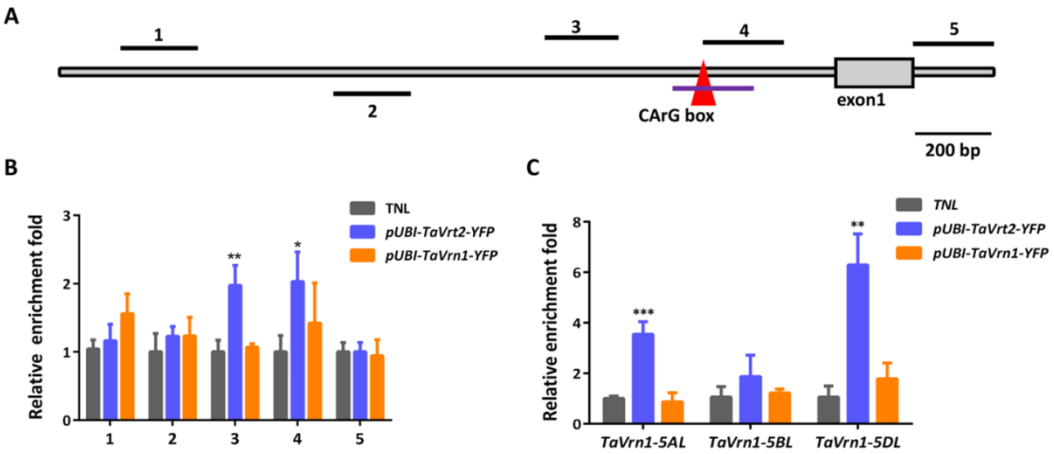

nph_16339_f6.png

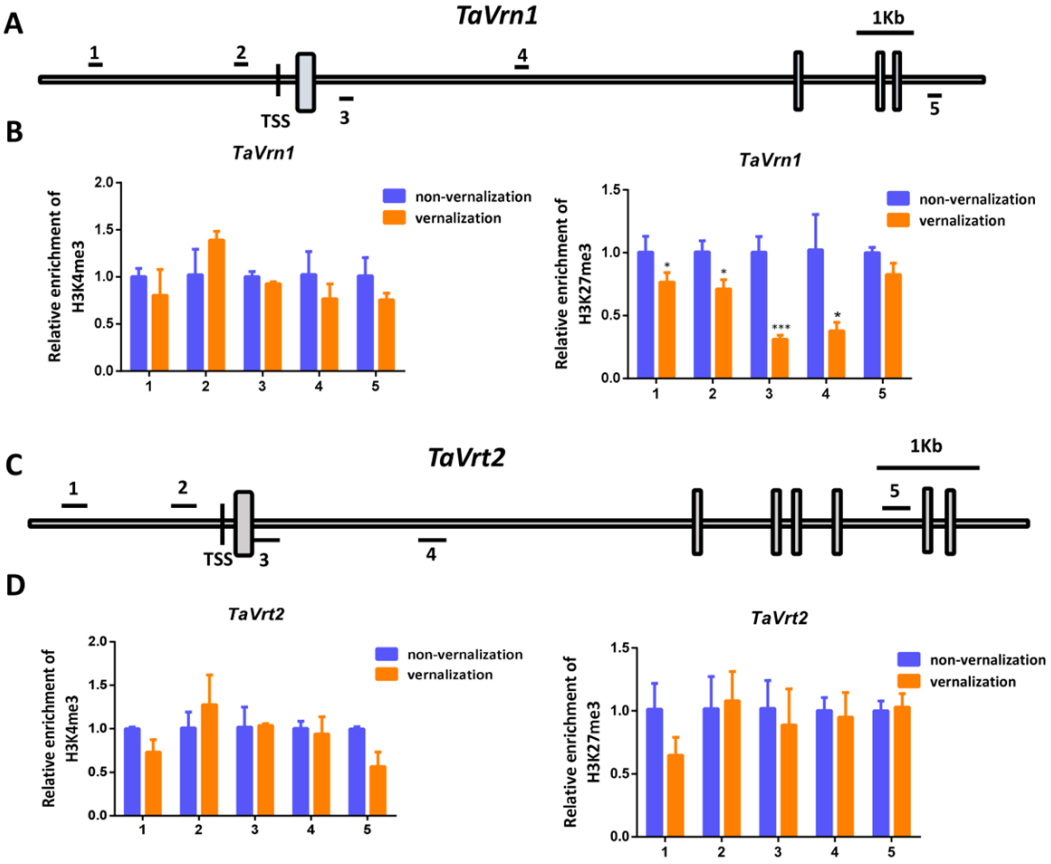

nph_16339_f7.png

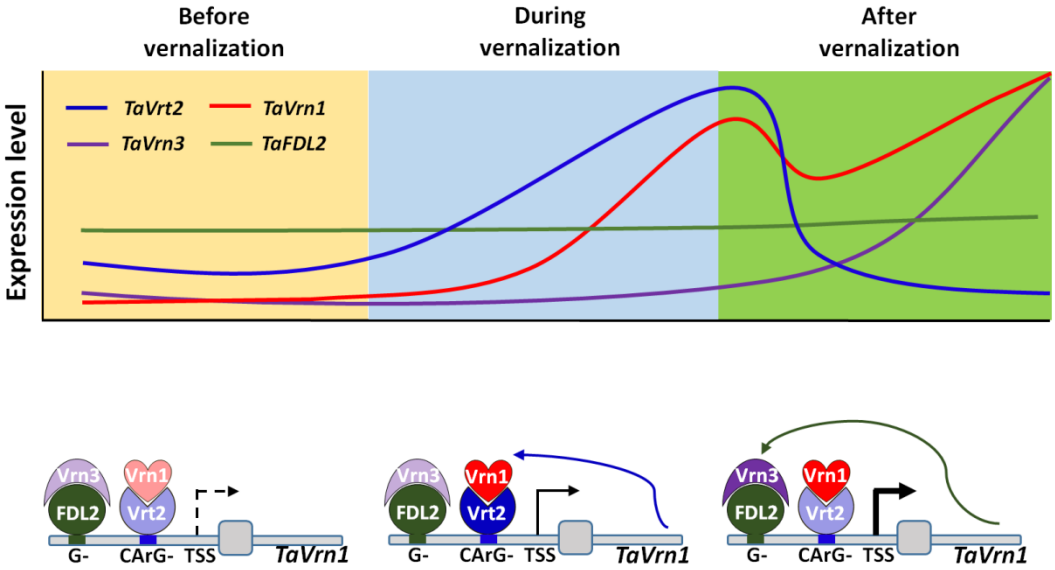

nph_16339_f8.png